Science Translational Medicine
AAAS

Supplementary Materials for

Precise genomic editing of pathogenic mutations in *RBM20* rescues dilated cardiomyopathy

Takahiko Nishiyama *et al.*

Corresponding author: Eric N. Olson, eric.olson@utsouthwestern.edu

Sci. Transl. Med. **14**, eade1633 (2022)
DOI: 10.1126/scitranslmed.ade1633

The PDF file includes:

Other Supplementary Material for this manuscript includes the following:

Supplementary Materials

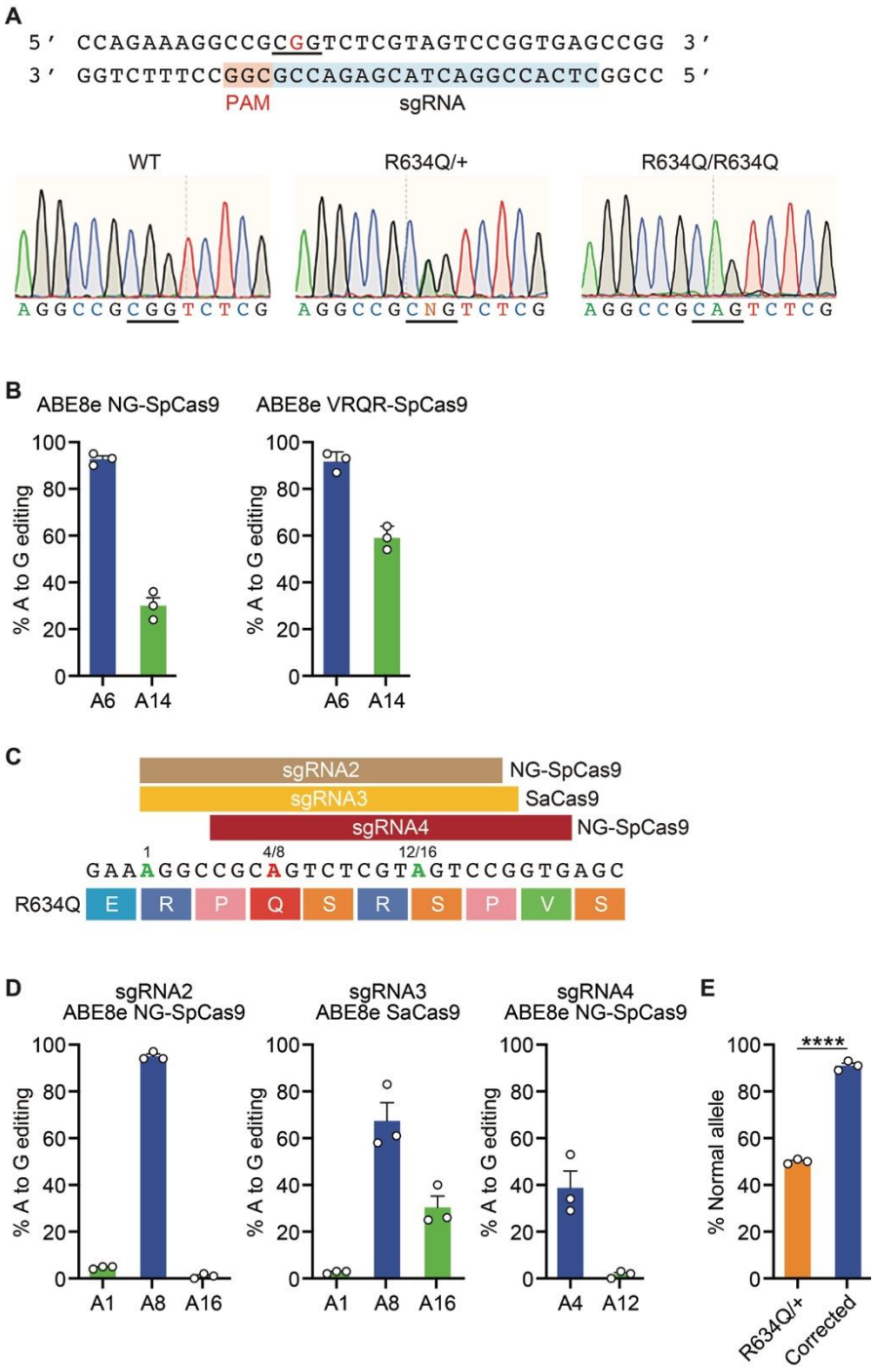

Fig. S1: Screening of sgRNAs with adenine base editors in iPSCs.

(**A**) Sequence of sgRNA (blue) targeting exon 9 of the human *RBM20* gene. PAM is highlighted in pink. Sanger sequence of the genomic region spanning the *RBM20*^{R634Q} mutation (underlined)

in wild type (WT), heterozygous (R634Q/+) and homozygous (R634Q/R634Q) iPSC lines. (**B**) Percentage of adenine (A) to guanine (G) editing in R634Q/R634Q iPSCs after ABE correction using sgRNA1 and ABE8e-NG-SpCas9 or ABE8e-VRQR-SpCas9. A6 is on-target site (blue). A14 is bystander site (green). Data are expressed as mean ± SEM (n = 3). (**C**) Illustration showing the binding positions of sgRNA2, 3 and 4 in the region of the *RBM20*^{R634Q} mutation. On-target site (red) and bystander site (green) are indicated. (**D**) Percentage of adenine (A) to guanine (G) editing in R634Q/R634Q iPSCs after ABE correction using sgRNA2, 3 and 4 coupled with each ABE8e base editor. On-target site (blue). Bystander site (green). Data are expressed as mean ± SEM (n = 3). (**E**) Percentage of normal allele in heterozygous (R634Q/+) iPSCs before and after correction with sgRNA1 and ABEmax-VRQR-SpCas9. Data are expressed as mean ± SEM (n = 3). Unpaired two-tailed Student's t test was performed. P value ****P<0.0001.

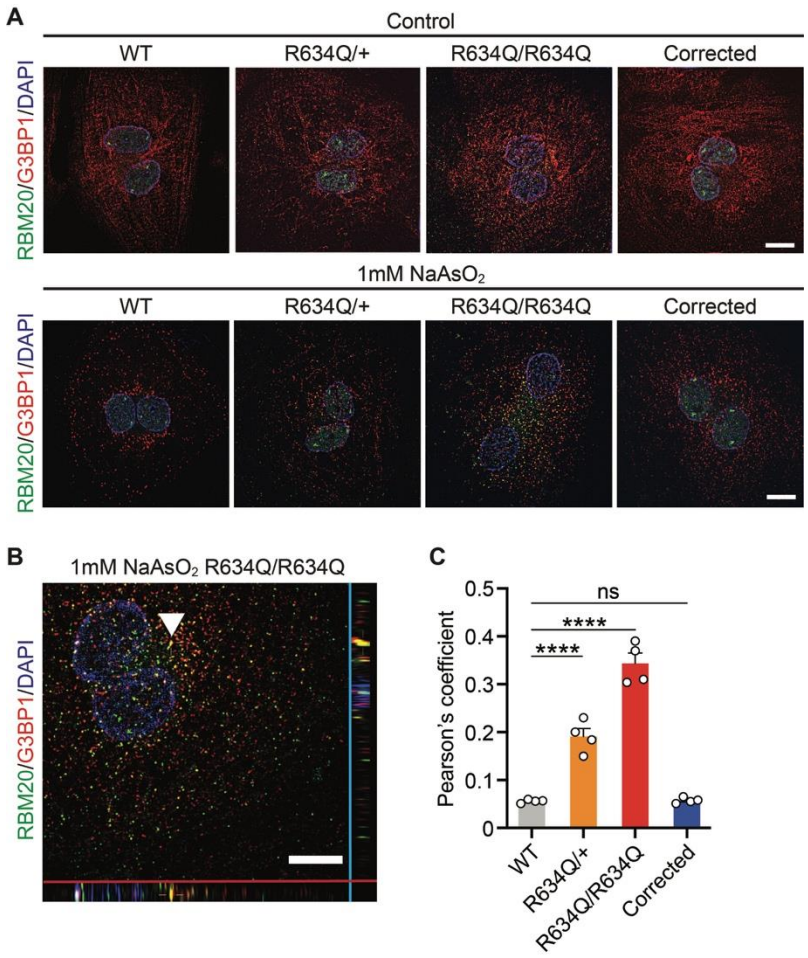

Fig. S2: RBM20^{R634Q} granules co-localized with stress granules in iPSC-derived cardiomyocytes.

(**A**) Immunostaining showing the distribution of RBM20 and G3BP stress granule assembly factor 1 (G3BP1) under normal and stress (1mM $NaAsO_2$) conditions. G3BP1, which is a marker for stress granules, expressed diffusely in cytoplasm under normal conditions. Under acute stress conditions, G3BP1 formed puncta (stress granules). DAPI denotes nuclei (blue). Scale bar, 10 μm. (**B**) RBM20^{R634Q} granules co-localized with stress granules are indicated by white arrowhead. Scale bar, 10 μm. (**C**) Co-localization of RMB20 and G3BP1 was measured by Pearson's coefficient. Data are expressed as mean ± SEM (n = 4). One-way ANOVA with Tukey's multiple comparisons test was performed. P value ****P<0.0001.

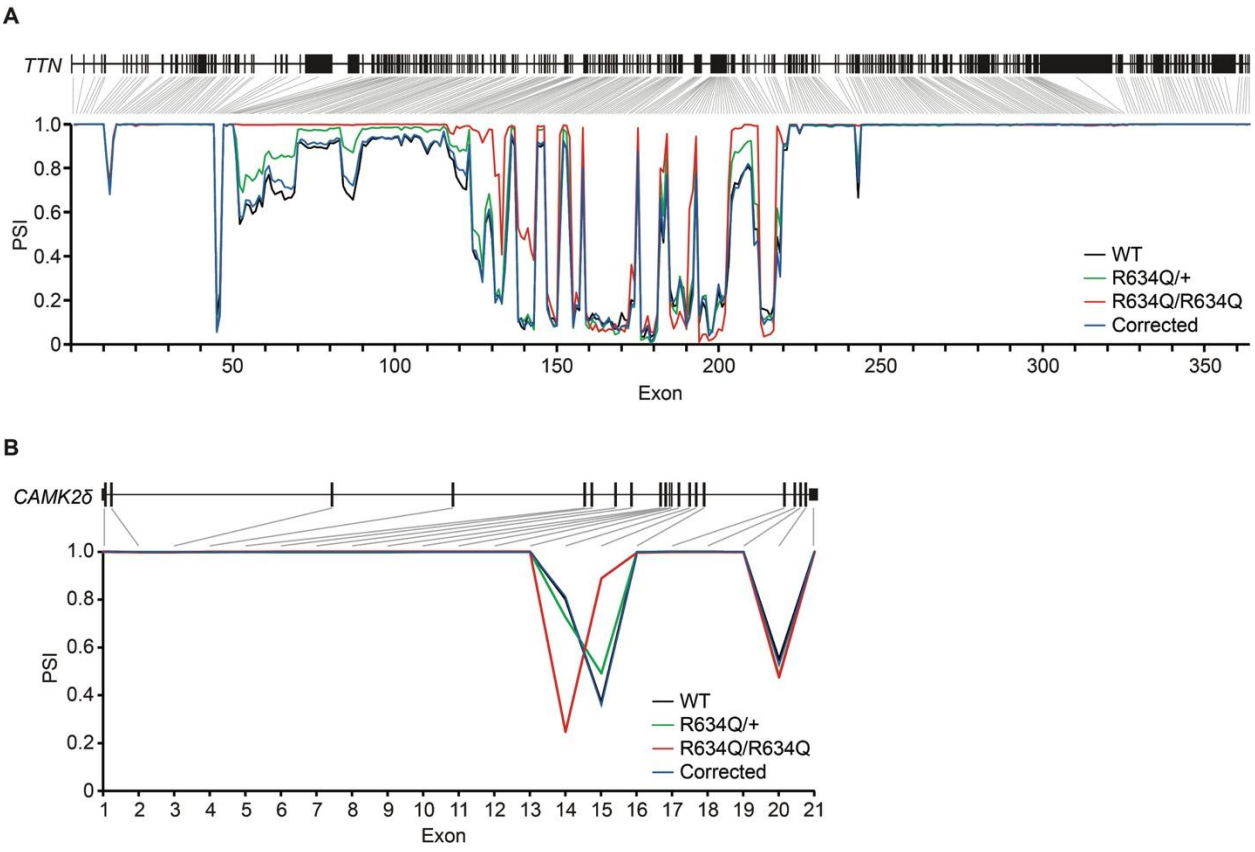

Fig. S3: Correction of alternative splicing of *TTN* and *CAMK2δ* genes in *RBM20*^{R634Q} iPSC-CMs after adenine base editing.

(**A**) and **(B**) Splicing pattern of the *TTN* (A) and *CAMK2δ* (B) genes as measured by percent spliced in (PSI) indicates exon-inclusion ratio. Recovery of splicing was seen in ABE-corrected R634Q/R634Q iPSC-CMs.

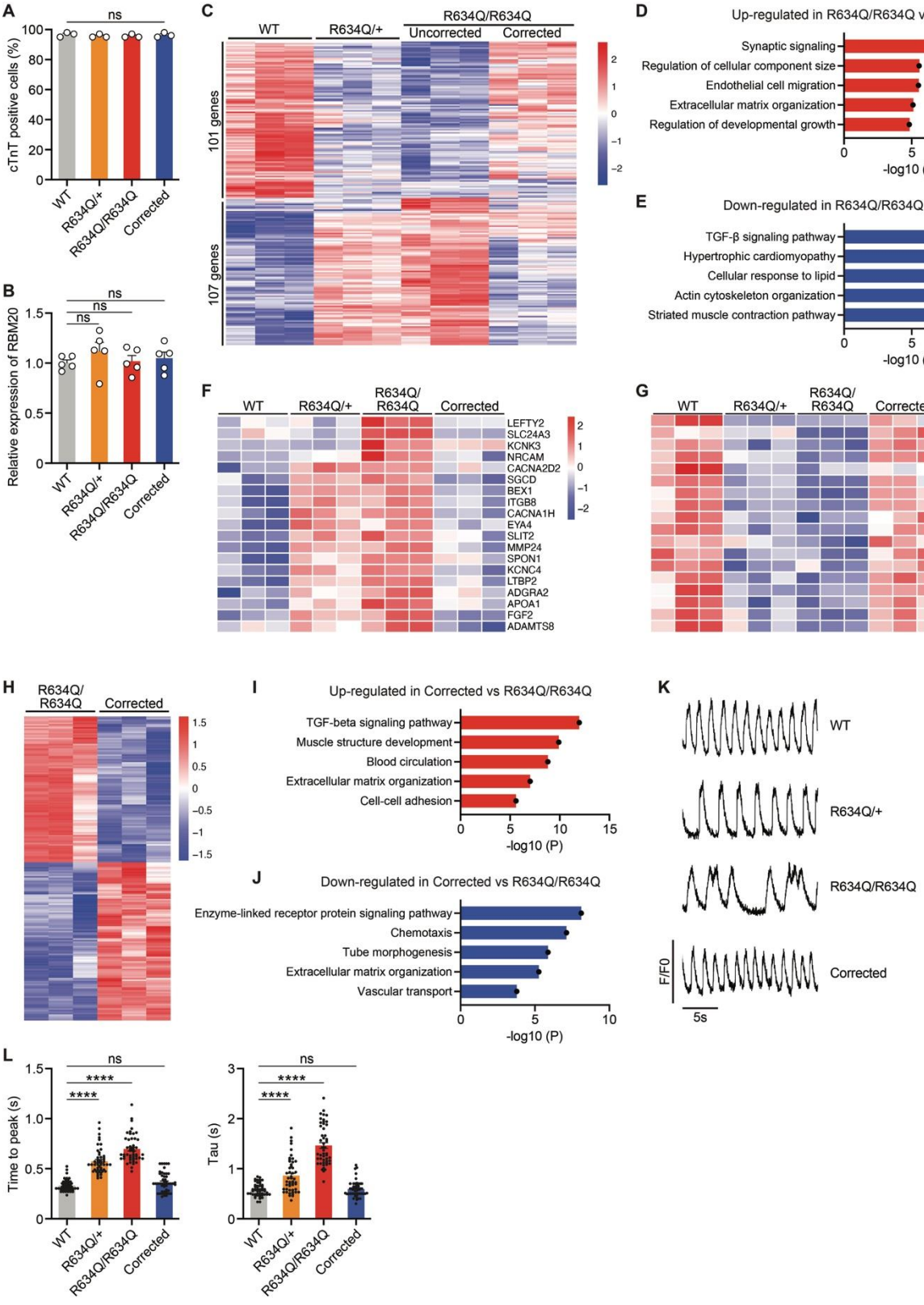
A
cTnT positive cells (%)
ns
WT
R634Q/+
R634Q/R634Q
Corrected
B
Relative expression of RBM20
ns
C
WT
R634Q/+
R634Q/R634Q
Uncorrected
Corrected
101 genes
107 genes
D
Up-regulated in R634Q/R634Q vs WT
Synaptic signaling
Regulation of cellular component size
Endothelial cell migration
Extracellular matrix organization
Regulation of developmental growth
-log10 (P)
E
Down-regulated in R634Q/R634Q vs WT
TGF-β signaling pathway
Hypertrophic cardiomyopathy
Cellular response to lipid
Actin cytoskeleton organization
Striated muscle contraction pathway
-log10 (P)
F
R634Q/ R634Q
LEFTY2
SLC24A3
KCNK3
NRCAM
CACNA2D2
SGCD
BEX1
ITGB8
CACNA1H
EYA4
SLIT2
MMP24
SPON1
KCNC4
LTBP2
ADGRA2
APOA1
FGF2
ADAMTS8
G
CASQ2
FBXO32
ID3
FBN1
ACTB
ACTA2
ITGA7
TPM2
FBLIM1
MYH14
SGCG
MYH6
LMOD3
ID2
TGFB2
BMP2
SMAD6
SMAD7
H
I
Up-regulated in Corrected vs R634Q/R634Q
TGF-beta signaling pathway
Muscle structure development
Blood circulation
Extracellular matrix organization
Cell-cell adhesion
J
Down-regulated in Corrected vs R634Q/R634Q
Enzyme-linked receptor protein signaling pathway
Chemotaxis
Tube morphogenesis
Extracellular matrix organization
Vascular transport
K
F/F0
5s
L
Time to peak (s)
Tau (s)
****

Fig. S4: Adenine base editing of R634Q/R634Q iPSC-CMs restored gene expression and calcium handling.

(**A**) Percentage of cardiac troponin T positive CMs in each group at day 40 post-differentiation (*n* = 3). One-way ANOVA with Tukey's multiple comparisons test was performed. (**B**) *RBM20* mRNA expression was quantified by qRT-PCR. Data are expressed as mean ± SEM (*n* = 5). One-way ANOVA with Tukey's multiple comparisons test was performed. (**C**) Heatmap showing differentially regulated gene expression of wild type (WT), R634Q/+, R634Q/R634Q and ABE-corrected R634Q/R634Q iPSC-CMs. (**D**) and (**E**) Gene Ontology (GO) terms associated with the up- (D) and down-regulated genes (E) in R634Q/R634Q iPSC-CMs compared to WT iPSC-CMs. RNA-seq analysis was performed on three independent differentiated iPSC-CMs at day 40 after differentiation. (**F**) and (**G**) Heatmaps of selected genes related to cardiomyopathy.

(**H** to **J**) Heatmap showing differentially regulated gene expression (H) and GO terms associated with the up- (I) and down-regulated genes (J) in ABE-corrected R634Q/R634Q iPSC-CMs compared to R634Q/R634Q iPSC-CMs. (**K**) Representative calcium traces of each group. (**L**) Quantification of the calcium release phase by time to peak and calcium reuptake phase by tau (*n* = 50 cells in each group; quantification was performed across three independent differentiation groups). Data are shown as means ± SEM. One-way ANOVA with Tukey's multiple comparisons was performed. *P* value ****$P<0.0001$. ns: not significant.

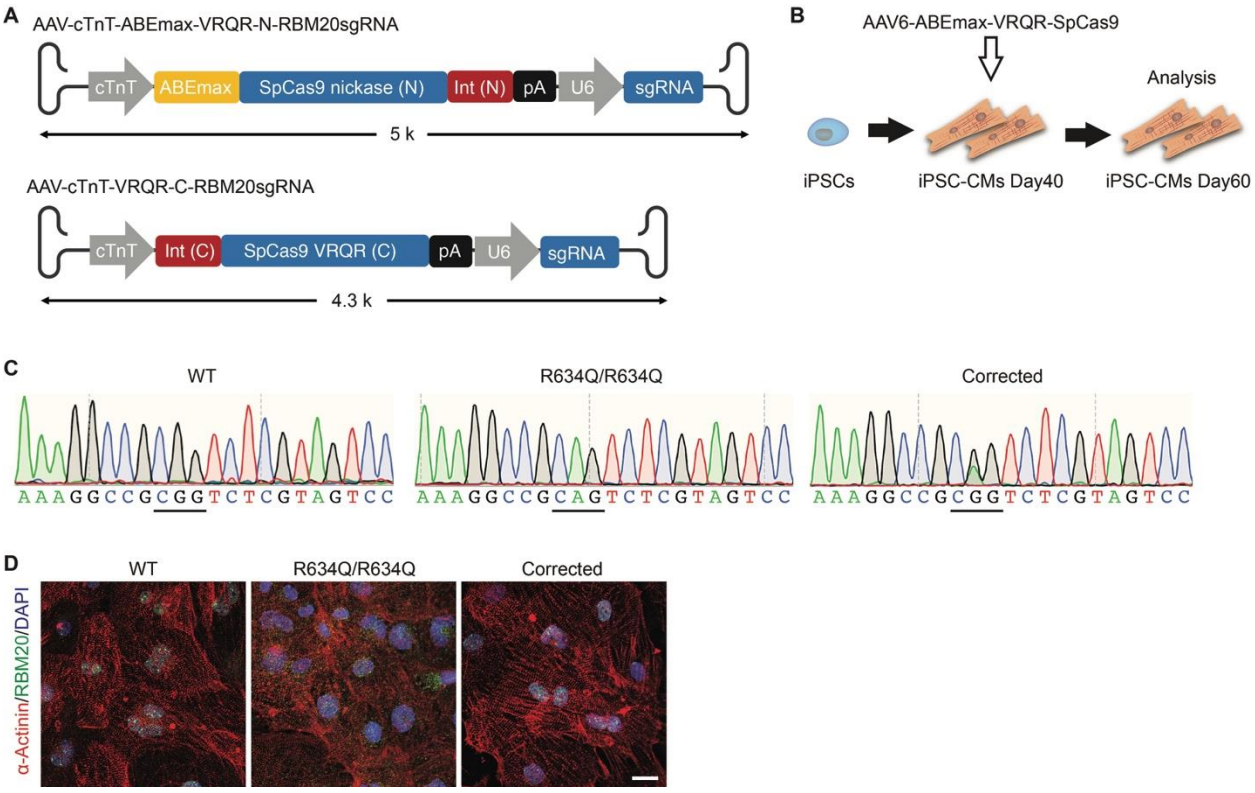

Fig. S5: ABE delivered by AAV6 restored the nuclear localization of RBM20 in differentiated R634Q/R634Q iPSC-CMs.

(**A**) Illustration of dual AAV vectors used to deliver ABE components to iPSC-CMs. ABEmax, VRQR-SpCas9 and inteins (Int) are driven by the cardiac troponin T promoter. sgRNA expression cassette is driven by U6 RNA polymerase III promoter. (**B**) Schematic showing experimental design of ABE delivery by AAV6 into differentiated iPSC-CMs. (**C**) Sanger sequence of the genomic region of the *RBM20*^{R634Q} mutation (underlined) in wild type (WT), uncorrected and ABE-corrected homozygous (R634Q/R634Q) iPSC-CMs. (**D**) Immunocytochemistry of WT, R634Q/R634Q and ABE-corrected R634Q/R634Q iPSC-CMs. α-Actinin (red), RBM20 (green) and DAPI (blue). Scale bar 20 μm.

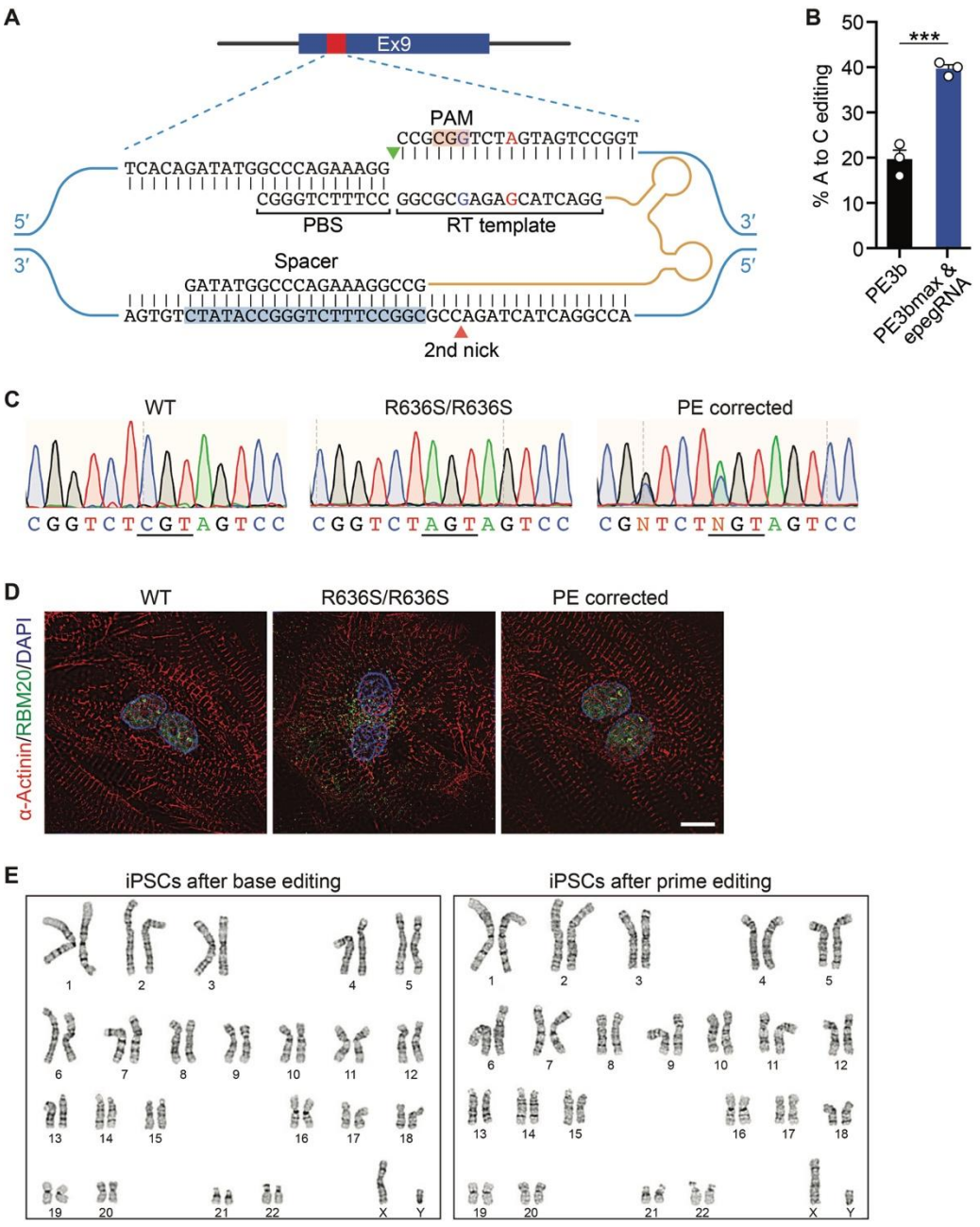

Fig. S6: Prime editing of the *RBM20*^{R636S} mutation in iPSCs.

(**A**) Illustration of the prime editing (PE) strategy for correction of the *RBM20*^{R636S} mutation. Prime editing guide RNA (pegRNA) contains a spacer, prime binding site (PBS, 11nt length) and reverse

transcriptase template (RT, 17nt length). The *RBM20*^{R636S} mutation and intended edited nucleotides are colored red. Silent mutation for disrupting the PAM is colored blue. The nicking site of pegRNA is indicated by a green arrowhead. The second nicking site of the sgRNA is indicated by a red arrowhead. (**B**) Percentage of adenine (A) to cytosine (C) editing after PE3b correction or PE3bmax with engineered pegRNA (epegRNA) correction in homozygous (R636S/R636S) iPSCs. Data are expressed as mean ± SEM (n = 3). Unpaired two-tailed Student's t test was performed. P value ***P<0.001. (**C)** Sanger sequence of the genomic region of the *RBM20*^{R636S} mutation (underlined) in wild type (WT), uncorrected and PE-corrected R636S/R636S iPSC lines. (**D**) Immunocytochemistry of WT, R636S/R636S and PE-corrected R636S/R636S iPSC-CMs. α-Actinin (red), RBM20 (green) and DAPI (blue). Scale bar, 10 μm. (**E**) Normal karyotype was observed in iPSCs after BE and PE genomic correction.

A

Base editing

Selected site	Sequence	PAM	Gene	Chromosome
RBM20 E9 On-target	GCCGCAGTCTCGTAGTCCGG	TGA	*RBM20*	10
Off-target-1	GCCGCCGCCTGGTAGTCCGG	CGA	*POC1B*	12
Off-target-2	GCAGCAGTCTTGTAGTCTGG	AGA	*ADGRV1*	5
Off-target-3	ACTGCAGTCTTGAAGTCCGG	TGA	Intergenic	8
Off-target-4	GCATCAGTCTCTTAGTCCTG	AGA	Intergenic	X
Off-target-5	GCCGCGGCCTGGTATTCCGG	CGA	*CENPC*	4
Off-target-6	GCCTCAGTCCCGTGGTCCTG	TGA	Intergenic	6
Off-target-7	GCCCCAGTCTCCTAGTCTGA	AGA	*ADGRL3*	4
Off-target-8	GCCTCAGTCTTGTGGTCCTG	TGA	Intergenic	11

Prime editing

Selected site	Sequence	PAM	Gene	Chromosome
RBM20 E9 On-target	GATATGGCCCAGAAAGGCCG	CGG	*RBM20*	10
Off-target-1	TAGATGACCCAGAAAGGCCA	CGG	Intergenic	4
Off-target-2	GAAACAGCCCAGAAAGGCCC	TGG	Intergenic	15
Off-target-3	GATCTGGCTCAGAAAGGCCA	AGG	Intergenic	1
Off-target-4	GATATGGCCCAAAGAGACCT	TGG	*GPR137B*	7
Off-target-5	GATATGCCCTAGAGAGACCG	TGG	Intergenic	21
Off-target-6	TGTATGGCCCAGGAAGGACG	CGG	*PDE9A*	13
Off-target-7	TACATTGCCCAGAAAGGCCA	AGG	*ATP11A*	17
Off-target-8	AATATGGACAAGAAAGGCAG	AGG	Intergenic	17

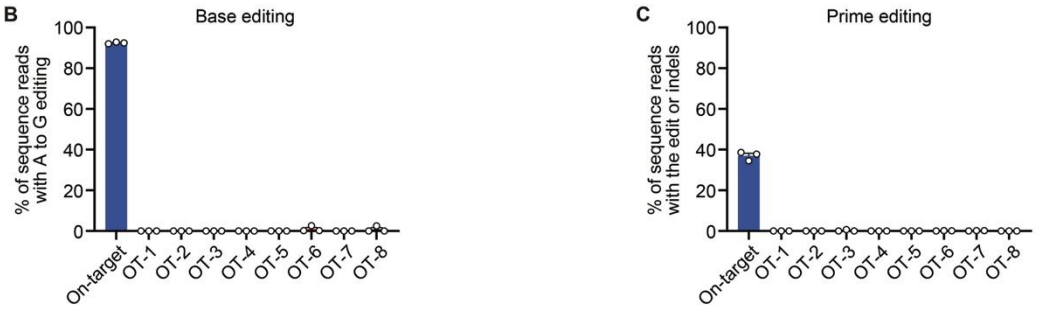

Fig. S7: Off-target analysis of base and prime editing in iPSCs.

(**A**) Genomic deep sequencing analysis on eight predicted off-target sites of BE and PE in iPSCs. (**B**) and (**C**) Percentage of editing determined by deep sequencing on the eight predicted off-target sites. Data are expressed as mean ± SEM (*n* = 3).

Fig. S8: Generating a knock-in mouse model carrying the *Rbm20*^{R636Q} mutation.

(**A**) Sequence of sgRNA (blue) targeting exon 9 of the *Rbm20* gene for generating a knock-in mouse model carrying the *Rbm20*^{R636Q} mutation. PAM is highlighted in pink. (**B**) Illustration showing the nucleotide and amino acid sequences around the genomic region of the *Rbm20*^{R636Q} mutation. Nucleotides shown in red are the knock-in *Rbm20*^{R636Q} mutation. Sanger sequence of the genomic region of the *Rbm20*^{R636Q} mutation in wild type (WT), heterozygous (R636Q/+) and homozygous (R636Q/R636Q) mice.

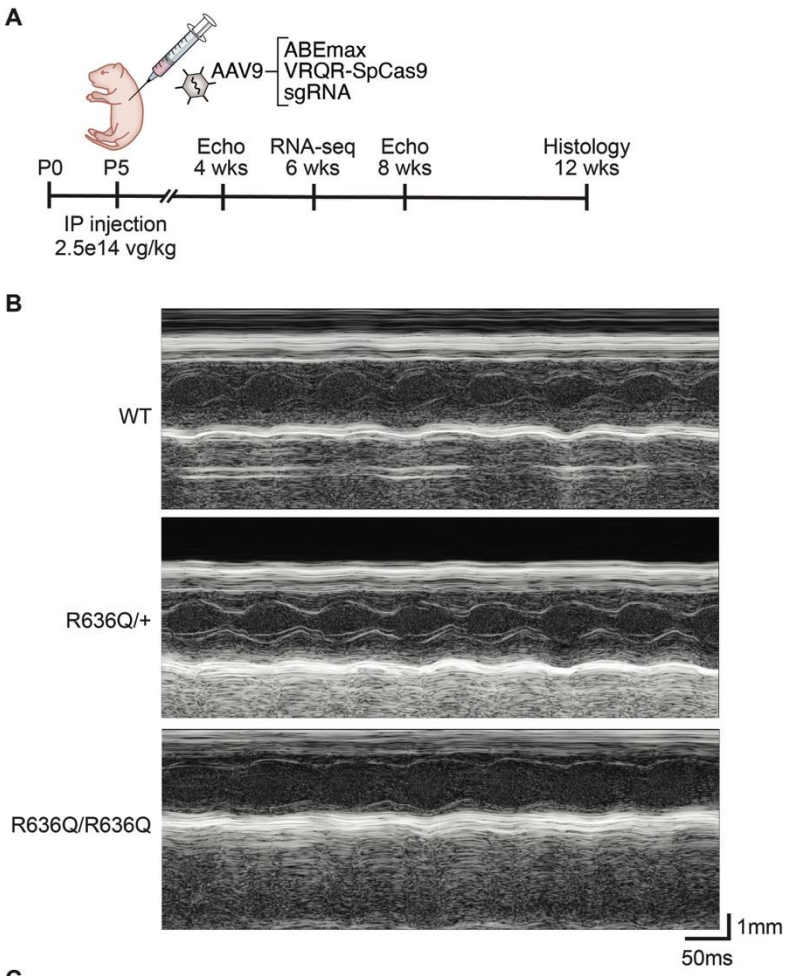
A
AAV9
ABEmax
VRQR-SpCas9
sgRNA
P0
P5
Echo
4 wks
RNA-seq
6 wks
Echo
8 wks
Histology
12 wks
IP injection
2.5e14 vg/kg
B
WT
R636Q/+
R636Q/R636Q
1mm
50ms
C
% FS
LVIDd (mm)
LVIDs (mm)
ns
****
**
WT
R636Q/+
R636Q/R636Q
D
WT
R636Q/+
R636Q/R636Q

Fig. S9: Cardiac dysfunction in postnatal *Rbm20*^{R636Q} mice and strategy for ABE correction. (**A**) Experimental design for systemic delivery of AAV9 with ABE components. R636Q/R636Q mice were injected intraperitoneally with 2.5 x 10^{14} vg/kg of total AAV9 components at postnatal day 5 (P5). Time points of analyses are indicated. (**B**) M-mode echocardiographic tracings of WT, R636Q/+ and R636Q/R636Q mice at P5. (**C**) Fractional shortening (FS), left ventricular end diastolic (LVIDd) and systolic (LVIDs) diameters measured by echocardiography. Data are expressed as mean ± SEM (*n* = 5-6 per genotype). One-way ANOVA with Tukey's multiple comparisons was performed. *P* value ***P*<0.01 and *****P*<0.0001. ns: not significant. (**D**) H&E staining of four-chamber heart histological sections from WT, R636Q/+ and R636Q/R636Q mice at P5. Scale bar, 1 mm.

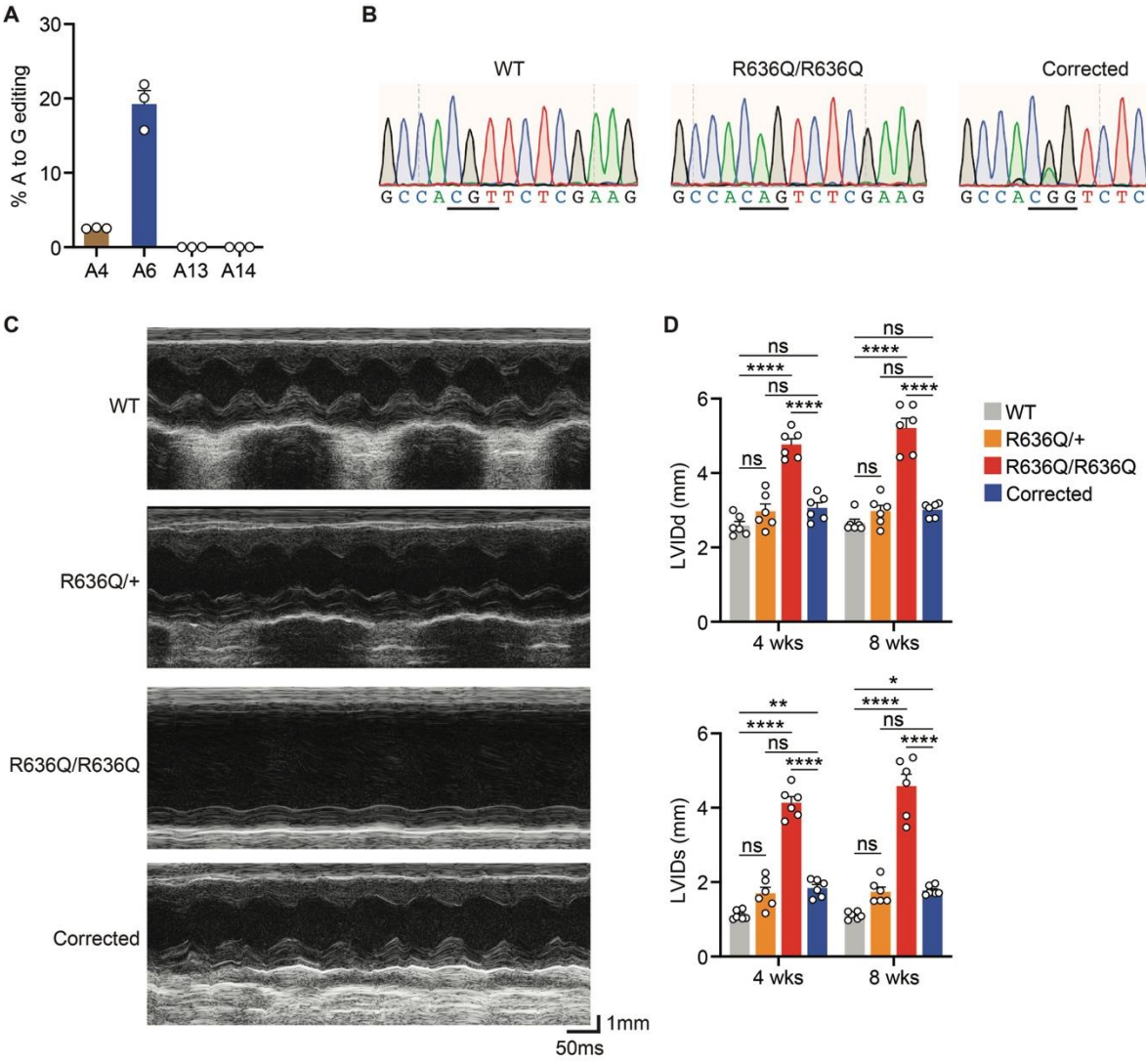

Fig. S10: Correction of the *Rbm20*^{R636Q} mutation by adenine base editing in vivo.

(**A**) Percentage of adenine (A) to guanine (G) editing determined by deep sequencing in DNA from hearts of ABE-corrected R636Q/R636Q mice at 6-weeks post-ABE correction. A6 is on-target site (blue). A14 is bystander site (green). A4 and A13 are silent mutations (brown). Data are expressed as mean ± SEM (n = 3). (**B**) Sanger sequencing showing the region of the *Rbm20*^{R636Q} mutation of heart cDNA in wild type (WT), homozygous (R636Q/R636Q) and ABE-corrected R636Q/R636Q (Corrected) mice. (**C**) M-mode echocardiographic tracings of WT, heterozygous (R636Q/+), R636Q/R636 and ABE-corrected R636Q/R636Q mice at 8-weeks post-ABE correction. (**D**) Left

ventricular end diastolic (LVIDd) and systolic (LVIDs) diameters measured by echocardiography at 4- and 8-weeks after ABE correction in WT, R636Q/+, R636Q/R636Q and Corrected mice. Data are expressed as mean ± SEM (n = 6 per group). Two-way ANOVA with Tukey's multiple comparisons test was performed. P value *P<0.05, **P<0.01 and ****P<0.0001. ns: not significant.

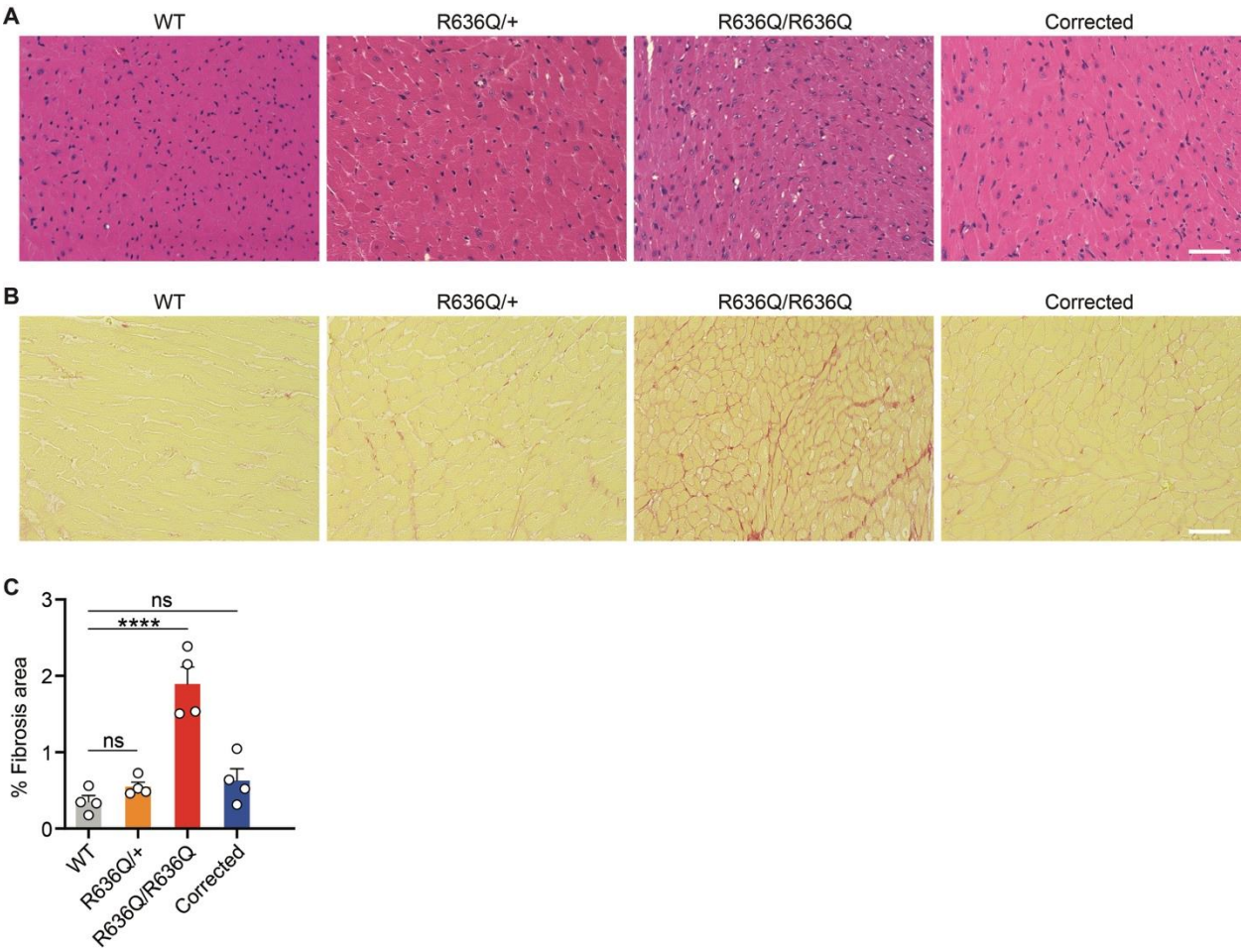

Fig. S11: Histological analysis of mouse hearts before and after ABE correction.

(**A**) H&E staining and (**B**) Picrosirius red staining of left ventricle in WT, R636Q/+, R636Q/R636Q and ABE-corrected R636Q/R636Q mice at 12-weeks after ABE correction. Scale bar, 50 μm. (**C**) Quantification of fibrosis area as determined by picrosirius red staining. Data are expressed as mean ± SEM (*n* = 4 per group). One-way ANOVA with Tukey's multiple comparisons test was performed. *P* value ****$P<0.0001$. ns: not significant.

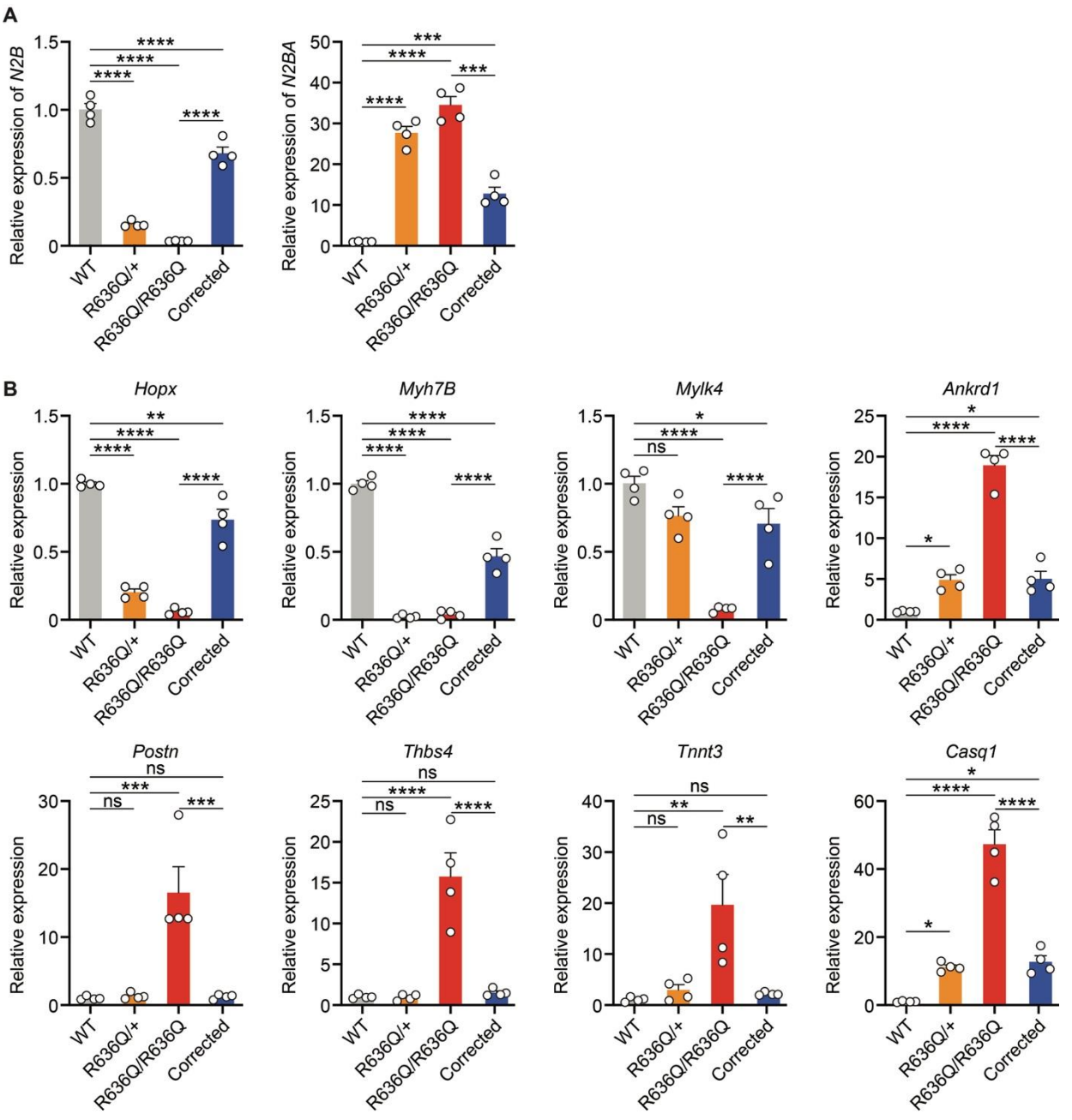

Fig. S12: Adenine base editing partially restored the alternative splicing and gene expression in vivo.

(**A**) Relative expression of the N2B isoform and the N2BA isoform of the titin (*Ttn*) gene was quantified by qRT-PCR in hearts of wild type (WT), heterozygous (R636Q/+), homozygous (R636Q/R636Q) and ABE-corrected R636Q/R636Q (Corrected) mice at 6-weeks after ABE

correction. Data are expressed as mean ± SEM (n = 4 per group). One-way ANOVA with Tukey's multiple comparisons test was performed. P value ***P<0.001 and ****P<0.0001. (**B**) Relative expression of selected genes quantified by qRT-PCR. Data are expressed as mean ± SEM (n = 4 per group). One-way ANOVA with Tukey's multiple comparisons test was performed. P value *P<0.05, **P<0.01, ***P<0.001 and ****P<0.0001. ns: not significant.

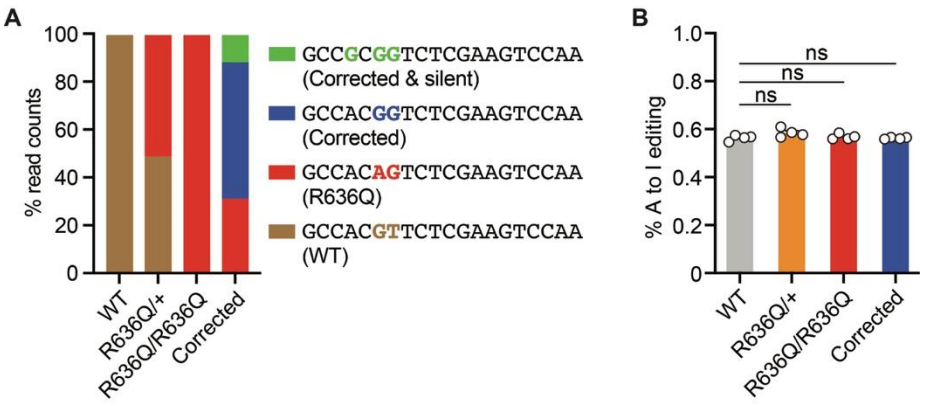

Fig. S13: Analysis of edited read counts and RNA A-to-I editing by RNA-seq.

(**A**) Percentage of read counts in the region of sgRNA sequence in hearts of WT, R636Q/+, R636Q/R636Q and ABE-corrected R636Q/R636Q mice at 6-weeks after ABE correction. (*n* = 4 per genotype). (**B**) Transcriptome-wide cellular levels of RNA A-to-I editing in WT, R636Q/+, R636Q/R636Q and Corrected mice at 6-weeks after ABE correction. Data are expressed as mean ± SEM (*n* = 4 per group). One-way ANOVA with Tukey's multiple comparisons test was performed. ns: not significant.

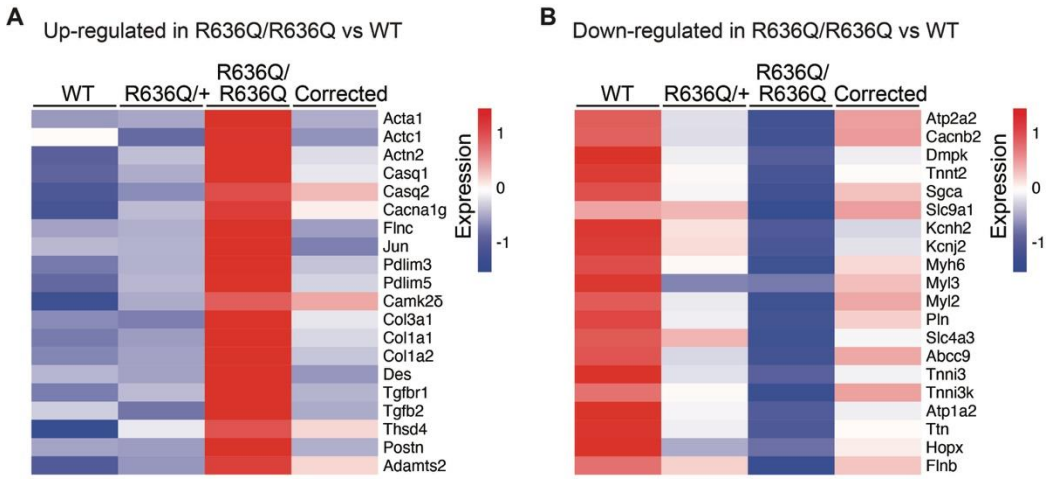

Fig. S14: Analysis of dysregulated genes in R636Q/R636Q compared to WT hearts.

Heatmap showing expression of selected (**A**) up- and (**B**) down-regulated genes in R636Q/R636Q compared to WT hearts.

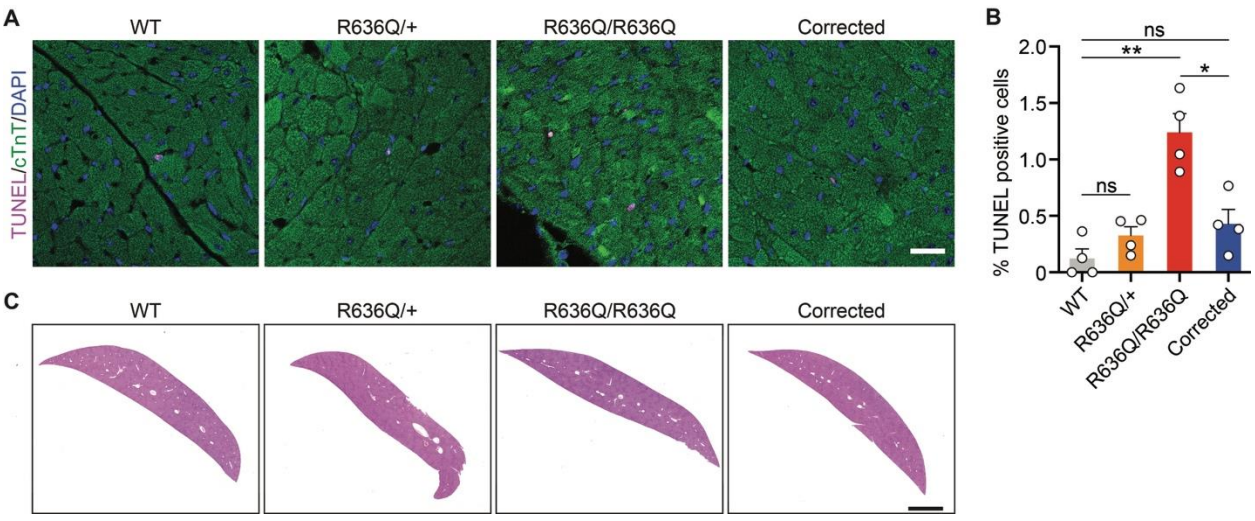

Fig. S15: No adverse events were observed in heart and liver following ABE-correction using AAV9 delivery system.

(**A**) Representative images showing TUNEL staining on heart sections from wild type (WT), heterozygous (R636Q/+), homozygous (R636Q/R636Q) and ABE-corrected R636Q/R636Q (Corrected) mice at 12-weeks after ABE correction. Scale bar, 20 μm. (**B**) Quantification of TUNEL positive cells in WT, R636Q/+, R636Q/R636Q and Corrected mice. Data are expressed as mean ± SEM (n = 4 per genotype). One-way ANOVA with Tukey's multiple comparisons test was performed. P -value *P<0.05 and **P<0.01. ns: not significant. (**C**) H&E staining of liver from WT, R636Q/+, R636Q/R636Q and Corrected mice at 12-weeks after ABE correction. Scale bar, 2 mm.

Table S1. Base editing single guide RNAs (sgRNAs) for correction of the *RBM20*^{R634Q} mutation.

Base editing sgRNA	sgRNA sequence	PAM	Cas9
sgRNA1	GCCGCAGTCTCGTAGTCCGG	TGA	NG- or VRQR-SpCas9
sgRNA2	AGGCCGCAGTCTCGTAGTCC	GG	NG-SpCas9
sgRNA3	AGGCCGCAGTCTCGTAGTCCG	GTGAGC	SaCas9
sgRNA4	CGCAGTCTCGTAGTCCGGTG	AG	NG-SpCas9

Table S2. List of primers and single-stranded oligodeoxynucleotides used in this study.

Primer function	Primer name	Primer sequence
Generating iPSCs (*RBM20*^{R634Q})	R634Q-sgRNA-FW	CACCGCTCACCGGACTACGAGACCG
	R634Q-sgRNA-RV	AAACCGGTCTCGTAGTCCGGTGAGC
	RBM20-Ex9-FW	GCCAGTGCTGTGCTTAGGA
	RBM20-Ex9-RV	TGGTGTTTGCGATCATGTGC
	ssODN-*RBM20*-R634Q	GTCTGTGTGTGGGTGGGGTGGGATGGGAGGTGT GAAGATTCTAAATCCTGCTCCTTGGCTCCCTCACA GATATGGCCCAGAAAGGCCGCAGTCTCGTAGTCC GGTGAGCCGGTCACTCTCCCCGAGG
Base editing sgRNAs (*RBM20*^{R634Q})	R634Q-sgRNA1-FW	CACCGCCGCAGTCTCGTAGTCCGG
	R634Q-sgRNA1-RV	AAACCCGGACTACGAGACTGCGGC
	R634Q-sgRNA2-FW	CACCGAGGCCGCAGTCTCGTAGTCC
	R634Q-sgRNA2-RV	AAACGGACTACGAGACTGCGGCCTC
	R634Q-sgRNA3-FW	CACCGAGGCCGCAGTCTCGTAGTCCG
	R634Q-sgRNA3-RV	AGACCGGACTACGAGACTGCGGCCTC
	R634Q-sgRNA4-FW	CACCGCGCAGTCTCGTAGTCCGGTG
	R634Q-sgRNA4-RV	AAACCACCGGACTACGAGACTGCGC
Human qRT-PCR	qRT-18SrRNA-FW	ACCGCAGCTAGGAATAATGGA
	qRT-18SrRNA-RV	GCCTCAGTTCCGAAAACCA
	qRT-TTN-N2B-FW	CCAATGAGTATGGCAGTGTCA
	qRT-TTN-N2B-RV	TACGTTCCGGAAGTAATTTGC
	qRT-TTN-N2BA-FW	ATCCTGAGAACCCAGGTGGT
	qRT-TTN-N2BA-RV	GGTTGGTGGATATGCCTCTGT
BE Off-target	BE OT1-FW	TTTGTTGAGGGCAGAGCCAA
	BE OT1-RV	TGGCACTCTTTGCTTGGTGA
	BE OT2-FW	GACTCTCTGTGGGCCTTCAAAGATGGA
	BE OT2-RV	TATTGGCGCTCGTCTGCCCAATCTC
	BE OT3-FW	CTTTCCTGACTACTTCCCTGGT
	BE OT3-RV	GAGTCTGGCAGTGGAACAAGA
	BE OT4-FW	GCAACTTGGCAAAGGGAAGAAAAACA
	BE OT4-RV	CAGAGTACCACTGCCTACCCACTACAA
	BE OT5-FW	GCATGTGTCTCCGGGTTCAA
	BE OT5-RV	GCGGCTTTCCCACTGAAATC
	BE OT6-FW	TGAACTGGACCCCCGAGGTGTAGCC
	BE OT6-RV	TTTCCTAAGAGTCGGTCGGCTTGAG
	BE OT7-FW	ATCCTTTGGGTCCAACCAGC
	BE OT7-RV	AGAGCACTTGGATAGTTGGCT
	BE OT8-FW	CCGGTTGATCTCAAAACCCTG
	BE OT8-RV	GGGAGACTGTTGGGAAGATA
PE Off-target	PE OT1-FW	GCACTCCCTGGATCCTCACAG
	PE OT1-RV	TGCCTCTAGACAGACATGTCGG
	PE OT2-FW	GGTAGAGCCATGATCTGAACCC
	PE OT2-RV	CTCCAAAGTTTGGCCAAATGACA
	PE OT3-FW	CCGAGTCACAGCCCACAACA
	PE OT3-RV	AGGCTGCCAACATCTCAGGAG
	PE OT4-FW	CCAGCTCTAGACATGCCACTG
	PE OT4-RV	GGAGCCGGGTAGACAAAGTT
	PE OT5-FW	GTCAAAACCTGGGTGGGGCA
	PE OT5-RV	CCAGCAAATGCCAGGAATCCT
	PE OT6-FW	TGAGCCAAGAGCTGCAGAGC

	PE OT6-RV	GAGGAACAGAGGACGCCAGA
	PE OT7-FW	GACAGAACGCGACTTCAGGA
	PE OT7-RV	TGCAGCTGGAAAGACTGAGG
	PE OT8-FW	GCAGATGGAATCAAACTGGTTGATC
	PE OT8-RV	CCATCCTAGATGAGAGTCTGTGCA
Generating iPSCs (*RBM20*^{R636S})	R636S-sgRNA-FW	CACCGACCGGCTCACCGGACTACG
	R636S-sgRNA-RV	AAACCGTAGTCCGGTGAGCCGGTC
	ssODN-*RBM20*-R636S	GTGTGGGTGGGGTGGGATGGGAGGTGTGAAGATT CTAAATCCTGCTCCTTGGCTCCCTCACAGATATGG CCCAGAAAGGCCGCGGTCTAGTAGTCCGGTGAGC CGGTCACTCTCCCCGAGGTCCCAC
PegRNA (PBS 11nt, RTT 17nt)	PegRNA-spacer-FW	CACCGATATGGCCCAGAAAGGCCGGTTTT
	PegRNA-spacer-RV	CTCTAAAACCGGCCTTTCTGGGCCATATC
	Scaffold-FW	AGAGCTAGAAATAGCAAGTTAAAATAAGGCTAGTC CGTTATCAACTTGAAAAAGTGGCACCGAGTCG
	Scaffold-RV	GCACCGACTCGGTGCCACTTTTTCAAGTTGATAAC GGACTAGCCTTATTTTAACTTGCTATTTCTAG
	PegRNA-FW	GTGCGGACTACGAGAGCGCGGCCTTTCTGGGC
	PegRNA-RV	AAAAGCCCAGAAAGGCCGCGCTCTCGTAGTCC
	PegRNA-2ndnick-FW	CACCGCTCACCGGACTACGAGAGCG
	PegRNA-2ndnick-RV	AAACCGCTCTCGTAGTCCGGTGAGC
EpegRNA (PBS 11nt, RTT 17nt)	EpegRNA-FW	GTGCGGACTACGAGAGCGCGGCCTTTCTGGGCTT GACGCGGTTCTATCTAGTTACGCGTTAAACCAACT AGAAA
	EpegRNA-RV	AAAATTTCTAGTTGGTTTAACGCGTAACTAGATAGA ACCGCGTCAAGCCCAGAAAGGCCGCGCTCTCGTA GTCC
ABE-SpCas9-variants-2A-GFP	AgeI-ABEmax-FW	TTTTTTTCAGGTTGGACCGGTGCCACCATGAAACG GACAGCC
	ABEmax-RV	GCCCACAGAGTTGGTGCCGAT
	SpCas9-FW	TCGGCACCAACTCTGTGGGC
	ApaI-SpCas9-RV	GCTGTTTCCCCTGGCCAGAGG
ABE8e-SaCas9-2A-GFP	Age1-ABE8e-FW	TTTTTTTCAGGTTGGACCGGTGCCACCATGAAACG GACAGCCG
	D10A-SaCas9-RV	TTGATGCTCTGGATGAAGCTCCGC
AAV-cTnT-ABEmax-VRQR-SpCas9-N and -C	XhoI-PacI-cTnT-F1	AGAAGAAATATAAGACTCGAGTTAATTAAGAGGTC GGGATAAAAGCAGTCTGGGC
	AgeI-cTnT-R1	CCGTTTCATGGTGGCACCGGTTCCCACGGAGCGG TGGGT
	U6-gRNA-F1	GGTGGGCTCTATGGGCGGCCGAGGGCCTATTTCC CATGATTCC
	XbaI-NotI-U6-gRNA-R1	GCTGGCGCGCCTTTTTCTAGAGCGGCCGCAAAAA AAGCACCGACTCGGTGC
	XhoI-U6-gRNA-F1	CGGTGGGCTCTATGGCTCGAGAGGGCCTATTTCC CATGATTCC
Generating a mouse model (*Rbm20*^{R636Q})	*Rbm20*-sgRNA-FW	CACCGCTCATTGGACTTCGAGAACG
	Rbm20-sgRNA-RV	AAACCGTTCTCGAAGTCCAATGAGC
	Rbm20-Ex9-FW	GGTAGAGGGCAGAGAGTGTCTTAGGG
	Rbm20-Ex9-RV	CCTTCGAGTCGCTCATCCAACTCAGC
	ssODN-*Rbm20*-R636Q	GTCTCCATCTGGGTGATGCAGGTTACGAGCTCTG CAGAGTCTAAACCCTGTCTCTTCCCTTCCTCCCAG GTATGGTCCAGAGCGGCCACagTCTCGAAGTCCAA TGAGCCGATCACTCTCCCCAAGA
	R636Q-sgRNA-FW	CACCGCCACAGTCTCGAAGTCCAA

Base editing sgRNA (*Rbm20*^{R636Q})	R636Q-sgRNA-RV	AAACTTGGACTTCGAGACTGTGGC
Mouse RT-PCR	Rbm20-FW	ATGGCTTACACAGAAGCCGC
	Rbm20-RV	CCTTCGAGTCGCTCATCCAA
Mouse qRT-PCR	qRT-mmu18SrRNA-FW	GTAACCCGTTGAACCCCATT
	qRT-mmu18SrRNA-RV	CCATCCAATCGGTAGTAGCG
	qRT-Ttn-N2B-FW	GGAGTACACCTGCAAAGCCT
	qRT-Ttn-N2B-RV	TGCGGCTTAGGTTCAGGAAG
	qRT-Ttn-N2BA-FW	GGAGTACACCTGCAAAGCCT
	qRT-Ttn-N2BA-RV	CCTTGGGCCTGGAGAGAAAG
	qRT-Ankrd1-FW	ATAAACGGACGGCACTCCAC
	qRT-Ankrd1-RV	CATCTGCGTTTCCTCCACGA
	qRT-Nppa-FW	KiCqStart SYBR Green Primers (Millipore Sigma)
	qRT-Nppa-RV	KiCqStart SYBR Green Primers (Millipore Sigma)
	qRT-Nppb-FW	KiCqStart SYBR Green Primers (Millipore Sigma)
	qRT-Nppb-RV	KiCqStart SYBR Green Primers (Millipore Sigma)
	qRT-Myh7B-FW	KiCqStart SYBR Green Primers (Millipore Sigma)
	qRT-Myh7B-RV	KiCqStart SYBR Green Primers (Millipore Sigma)
	qRT-Hopx-FW	KiCqStart SYBR Green Primers (Millipore Sigma)
	qRT-Hopx-RV	KiCqStart SYBR Green Primers (Millipore Sigma)
	qRT-Mylk4-FW	KiCqStart SYBR Green Primers (Millipore Sigma)
	qRT-Mylk4-RV	KiCqStart SYBR Green Primers (Millipore Sigma)
	qRT-Thbs4-FW	KiCqStart SYBR Green Primers (Millipore Sigma)
	qRT-Thbs4-RV	KiCqStart SYBR Green Primers (Millipore Sigma)
	qRT-Postn-FW	KiCqStart SYBR Green Primers (Millipore Sigma)
	qRT-Postn-RV	KiCqStart SYBR Green Primers (Millipore Sigma)
	qRT-Casq1-FW	KiCqStart SYBR Green Primers (Millipore Sigma)
	qRT-Casq1-RV	KiCqStart SYBR Green Primers (Millipore Sigma)
	qRT-TnnT3-FW	KiCqStart SYBR Green Primers (Millipore Sigma)
	qRT-TnnT3-RV	KiCqStart SYBR Green Primers (Millipore Sigma)

RBM20; RNA binding motif protein 20, Ex; Exon, sgRNA; single guide RNA, FW; forward, RV; reverse, ssODN; single-stranded oligodeoxynucleotide, OT; off-target, BE; base editing, PE; prime editing, ABE; adenine base editing, PegRNA; prime editing guide RNA, EpegRNA; engineered prime editing guide RNA, PBS; primer binding site, RTT; reverse transcriptase template, AAV; adeno associated virus, cTnT; cardiac troponin T, 18SrRNA; 18S ribosomal RNA, Ttn; titin, Ankrd1; ankyrin repeat domain 1, Nppa; natriuretic peptide A, Nppb; natriuretic peptide B, Myh7B; Myosin heavy chain 7B, HOPX; HOP homeobox, Mylk4; myosin light chain kinase family member 4, Thbs4; thrombospondin 4, Postn; periostin, Casq1; calsequestrin 1, TnnT3; troponin T3, fast skeletal type.

Data file S1. Raw data for all experiments where $n<20$.